Journal of Solid State Chemistry 183 (2010) 2932–2936

Contents lists available at ScienceDirect

Journal of Solid State Chemistry

journal homepage: www.elsevier.com/locate/jssc

The electrochemical performance of ordered mesoporous carbon/nickel compounds composite material for supercapacitor

Jicheng Feng, Jiachang Zhao, Bohejin Tang, Ping Liu, Jingli Xu *

College of Chemistry and Chemical Engineering, Shanghai University of Engineering Science, Shanghai 201620, China

ARTICLE INFO

Article history:
Received 17 June 2010
Received in revised form
5 September 2010
Accepted 28 September 2010
Available online 7 October 2010

Keywords:
Composite material
Nickel nitrate hydroxide hydrate
Electrochemical performance
Temperature

ABSTRACT

A series of high performance ordered mesoporous carbon/nickel compounds composites have been synthesized by a combination of incipient wetness impregnation and hydrothermal method for the first time. X-ray diffraction (XRD), N_2 adsorption/desorption isotherms and transmission electron microscopy (TEM) are used to characterize the composites derived at the hydrothermal temperature of 125, 150, 175, 200, 250, 275 and 300 °C. The formation of nanosized nickel compounds, fully inside the mesopore system, was confirmed with XRD and TEM. An N_2 adsorption/desorption isotherms measurements still revealed mesoporosity for the host/guest compounds. It is noteworthy that an OMC/nickel nitrate hydroxide hydrate composite (OMCN-150) exhibits more excellent performance. Based on the various hydrothermal temperatures of the composite, the capacitance of an OMCN-150 delivering the best electrochemical performance is about 2.4 (5 mV s^{-1}) and 1.5 (50 mV s^{-1}) times of the pristine OMC. The capacitance retention of an OMCN-150 is 96.1%, which indicates that the electrochemical performance of the supercapacitor is improved greatly, and represents novel research and significant advances in the field of electrode composite materials for supercapacitor.

1. Introduction

Electrochemical supercapacitors are becoming attractive energy storage devices for application involving high power and energy density as well as high cycle capacity requirements [1]. According to an energy storage mechanism, supercapacitors are divided into two categories, namely, electrical double-layer capacitors (EDLCs) and pseudocapacitors.

Following the report of Ryoo et al. [2], ordered mesoporous carbons (OMC) have rapidly attracted much attention in many applications [3–6], including as energy storage material, catalyst support and adsorbent, due to their high surface areas, ordered-arranged pore structures and narrow pore size distributions. However, the present application of the ordered mesoporous carbons only took advantage of its double-layer capacitance. Generally speaking, adding metal compounds into the electric double-layer electrodes is an effective way to enhance the specific capacitance [7,8]. It is reported that ordered mesoporous carbon can be used as the host material to prepare host–guest composite material by introducing metal compounds into its channel [9,10]. Recently, more and more researchers develop various alternatives as a replacement for RuO_2 and IrO_2, such as NiO_x [11–14], MnO_x [15], CoO_x [16], $Ni(OH)_2$ [17], etc, aiming to lower the cost of electrode material while using environmentally friendly materials. Among these candidates, $Ni(OH)_2$ and nickel oxide are known as promising electrode material for applications in energy/power storage devices, especially as supercapacitors. It is attractive in view of their low cost, well-defined electrochemical redox activity and the possibility of enhanced performance through different preparative methods [18–20], such as chemical liquid precipitation, electrodeposition, sol–gel technique and template synthesis method [12,13]. However, only few papers are reported for the capacitive behavior of the $Ni(OH)_2$ up to now [23,24].

Moreover the dependence of the hydrothermal temperature is of substantial practical significance in the preparation of composite electrode materials. So far, there is still no report on the supercapacitor fabricated with ordered mesoporous carbon and nickel compound nanocrystallites prepared by a combination of incipient wetness impregnation and hydrothermal treatment procedure to our best knowledge. More importantly, a completely novel electrode material for supercapacitor-nickel nitrate hydroxide hydrate is synthesized firstly. Nickel nitrate hydroxide hydrate appears to be a promising electrode material for pseudocapacitor, due to its excellent electrochemical performance, environmentally friendly and low cost. It is to be confirmed that it may open an opportunity to synthesize other novel electrode materials for supercapacitor.

In this research, the electrochemical performances of the composites were investigated in detail. The $OMC/Ni_2(NO_3)_2$

---

* Corresponding author. Fax: +86 21 67791220.
E-mail addresses: jinglixu@sues.edu.cn, fjc0422@163.com (J. Xu).

0022-4596/$ - see front matter © 2010 Elsevier Inc. All rights reserved.
doi:10.1016/j.jssc.2010.09.043

$(OH)_2 \cdot 2H_2O$ host–guest composite electrode material is expected to greatly improve the electrochemical properties of the supercapacitor.

2. Experimental

2.1. Synthesis of the composite

The synthesis of the host structure OMC was carried out using SBA-15 silica as the hard template and sucrose as the carbon source, following the synthesis procedure described as follows.

The preparation of the SBA-15 silica is based on the synthesis procedure first reported by Zhao et al. [25]. The calcinated SBA-15 was impregnated with an aqueous solution of sucrose containing sulfuric acid, similarly to the synthesis of CMK-1, except for the different amounts of the sulfuric acid and sucrose.

$Ni(NO_3)_2 \cdot 6H_2O$ (2.4889 g) was dissolved in distilled water (8 ml). Then, the amount of an OMC (1 g) was added to the above solution, stirred for 60 min. Hydrothermal treatment of the precursors was at different temperatures at 125, 150, 175, 200, 250, 275 and 300 °C for 2 h in autoclave. The composite synthesized at 150 °C was defined as an OMCN-150, and that of 125, 175, 200, 250, 275 and 300 °C was defined as OMCN-125, OMCN-175, OMCN-200, OMCN-250, OMCN-275 and OMCN-300, respectively.

2.2. Structural characterization

The pore characteristics of the obtained OMC and composites were measured on a Micromeritics (ASAP 2010) instrument, using nitrogen at 77 K. Mesopore size distributions were determined by Barrett–Joyner–Halenda (BJH) method. The X-ray diffractions (XRD) of the samples were performed on a diffraction meter (D/Max-rB) with Cu K_α radiation ($\lambda = 1.54056$ Å) and a graphite monochromator at 50 kV, 100 mA. Transmission electron micrographs (TEM) were taken on a JEOL-2010 microscope at an accelerating voltage of 200 kV.

Electrochemical characterization

In order to prepare the supercapacitor electrode, a mixture of composite, poly tetrafluoroethylene (PTFE) binder and BP2000 with the weight percent ratio of 75:20:5 was dispersed in alcohol and coated on a piece of foam nickel (1×1 cm^2), then pressed under the pressure of 10 MPa. The electrochemical properties of the composites were analyzed using a three-electrode configuration in aqueous 2.0 M KOH electrolyte. The Pt and saturated calomel electrode were used as the counter and reference electrode, respectively. Cyclic voltammetry was performed on a CHI660C instrument in the potential range −0.2 to 0.5 V (vs. SCE) with a scan rate from 5 to 200 mV s^{-1}. The specific capacitance (SC) was calculated by the following equation:

$$C = Q/m\Delta V \tag{1}$$

The charge (Q) is half of the integrated area of the CV curve; m and ΔV represent the mass of the electrode and the potential window, respectively.

3. Results and discussion

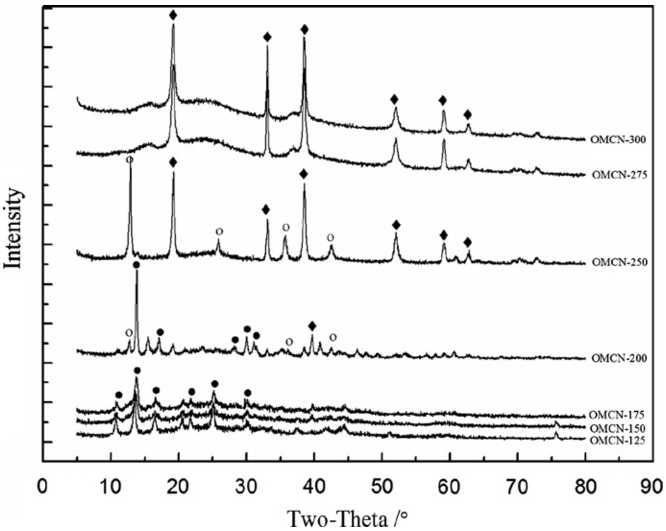

Fig. 1. XRD patterns of an OMCN-x (x=125, 150, 175, 200, 250, 275, 300) at different temperatures. Position of the peaks expected for the (●) $Ni_2(NO_3)_2(OH)_2 \cdot 2H_2O$, (●) $Ni_3(NO_3)_2(OH)_4$ and (◆) $Ni(OH)_2$.

The X-ray diffraction patterns recorded for these composites are shown in Fig. 1 as examples of the structural transformations taking place in the composites. It can be seen from the figure of an OMCN-300 that the peak profile has relatively strong intensity, which clearly indicates quite good crystallinity for an OMCN-300 obtained at 300 °C. These results agree reasonably well with the normal value for these compounds reported by JCPDS: 27–0952, 22–0752 and 14–0117. The peaks of the OMCN-250 can be indexed to both $Ni(OH)_2$ and $Ni_3(NO_3)_2(OH)_4$ peaks; $Ni(OH)_2$ is presented as a major phase and the peaks are sharper, which indicates the good crystallinity of the particles. $Ni_3(NO_3)_2(OH)_4$ is presented as a minor phase and the broadened peaks reveal the poorly crystalline nature of particles. When the temperature was further elevated to 275 °C, $Ni_3(NO_3)_2(OH)_4$ phase disappears, as expected, and the $Ni(OH)_2$ develops as the major phase. The patterns of the OMCN-x (x=125, 150, 175) composites show very broad diffraction peaks, but there are some changes. A new broad peak was observed at about 19° of an OMCN-200 that can be ascribed to $Ni(OH)_2$, and the most intense peak at 14° ascribed to $Ni_2(NO_3)_2(OH)_2 \cdot 2H_2O$. It is noteworthy that no $Ni(OH)_2$ phase appeared in an OMC framework for hydrothermal temperatures below 200 °C and no nickel oxides at all temperatures. Shanmugam et al. [26] have reported that the decomposition temperature of nickel nitrates in air and hydrogen environments is 307 ± 25 °C. However, the nickel compound was decomposed to $Ni(OH)_2$ while the hydrothermal temperature is 275 °C. The reason is possibly that the carbon framework and the high pressure may increase the surface energy of nickel nitrate, which would intensify and unsterilize the nickel compound nanocrystallites. Other papers have reported the synthesis of Fe_2O_3 nanoparticles within the pore system of mesoporous carbon CMK-1, without reduction [27]. When the hydrothermal temperature was further increased to 300 °C, the decomposition of $Ni(OH)_2$ proceeded, and thus a small fraction of $Ni(OH)_2$ was decomposed to nickel oxide. But none of the peaks of nickel oxide was found. The possible reaction for that is

$$NiO_X + H_2O \xrightarrow{High\ pressure} Ni(OH)_2$$

N_2 adsorption/desorption isotherms and pore size distributions of OMC and OMCN-150 are presented in Fig. 2, respectively. Although only OMC presents type IV isotherms individually according to the IUPAC classification, the volume adsorbed of N_2 decreases after nickel nitrate hydroxide hydrate loaded. The pore characteristics, viz. the Brunauer, Emmett and Teller (BET) surface

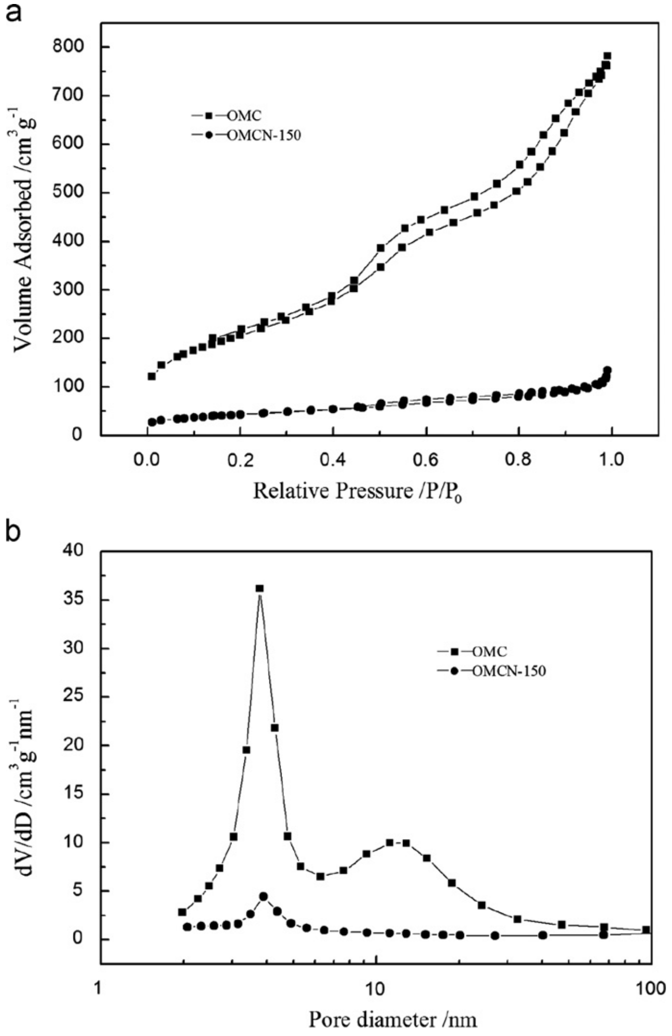

Fig. 2. N_2 adsorption/desorption isotherms (a) and pore size distributions (b) of OMC and OMCN-150.

Table 1
Pore characteristics of OMC and OMCN-150.

Sample	S_{BET} (m^2 g^{-1})	V_t (cm^3 g^{-1})	Mean pore size (nm)
OMC	745	1.14	5.57
OMCN-150	153	0.16	5.96

area, total pore volume and mean pore diameter determined from the N_2 adsorption and desorption isotherms are shown in Table 1. The parameters of porous texture are also found to decrease after the nickel nitrate hydroxide hydrate loaded, which resulted from the high degree of pore filling. The pore size distribution of an OMC is confirmed to be mesoporous, which is in good agreement with that deduced from the adsorption and desorption isotherms.

From the TEM images (Fig. 3), we can conclude the formation of the nickel nitrate hydroxide hydrate almost exclusively inside the mesopores of the host structure. The results demonstrate that the nickel compound crystallites were encapsulated in the wall of the OMC structure and did not block the mesochannel, which proved the preservation of the host structure during impregnation and hydrothermal treatment procedures. In addition, the filling of nickel nitrate hydroxide hydrate was fully loaded in the channel of OMC and the host–guest structure (the nominal weight ration of nickel oxide is 39 wt%).

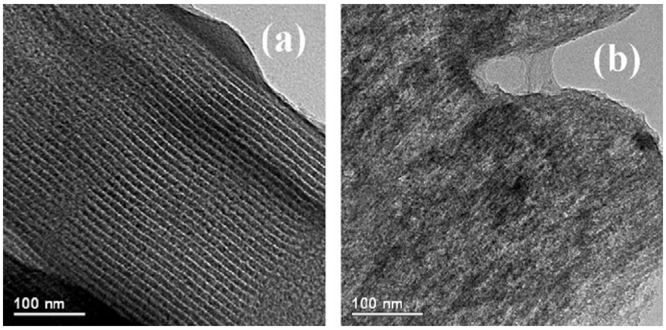

Fig. 3. TEM images of (a) the ordered mesoporous carbon (OMC) and (b) OMCN-150.

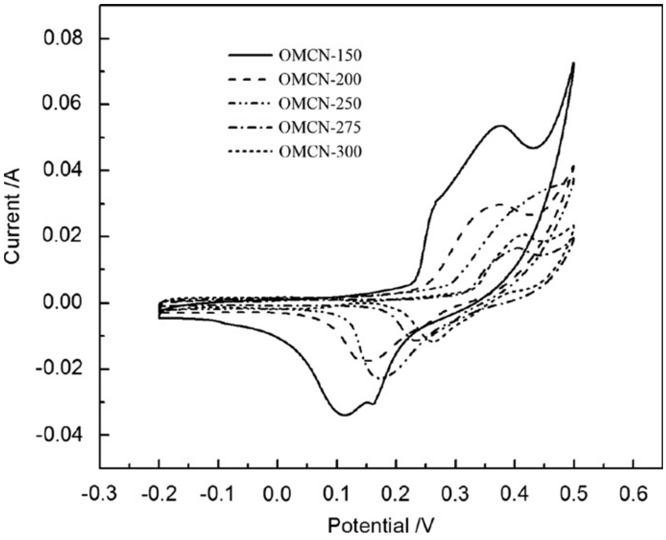

Fig. 4. Cyclic voltammogram for an electrode at a scan rate of 5 mV s^{-1} in 2 M KOH.

Fig. 4 presents the cyclic voltammetric behaviors of OMCN-*x* ($x=150$, 200, 250, 275, 300) electrodes at a sweep rate of 5 mV s^{-1}. The OMCN-150 electrode clearly shows faradic redox reactions, which are observed at 0.37 and 0.1 V with respect to the SCE reference electrode representing oxidation and reduction processes. All the electrodes basically show a shape similar to that of the $Ni(OH)_2$ electrode possessing the faradic redox behavior. Redox peak behaviors are observed at a wide range of voltage. The OMCN-275 composite electrode shows faradic redox reactions representing oxidation and reduction processes at 0.4 and 0.25 V, respectively. The composites demonstrated poorer electro chemical capacitance performance with the increase of the hydrothermal temperature from 150 to 300 °C. Moreover it is worth mentioning that the OMCN-150 was quite fit for the application to supercapacitor and rendered a voltage limit of the hybrid capacitor extending to 0.7 V. This is of great importance to the enhancement of specific energy density and practical commercial interest. Consequently, the electrochemical capacitance scale of the composite is much larger than that of the individual materials. From integrating the CV curve, the OMCN-150 composite electrode shows high specific capacitance (about 581 F g^{-1}) as a single electrode capacitance, while the capacitance of the OMCN-275 (OMC/$Ni(OH)_2$ composite) electrode is no more than 245 F g^{-1}. We can see from the CV curves that the OMCN-150 electrode shows the characteristics of a pseudo-capacitive electrode. This wider potential scope for the composite electrode results from textural characteristics

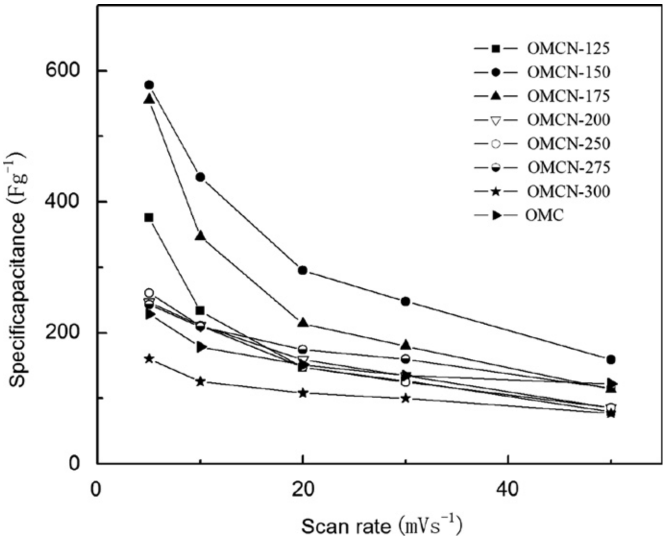

Fig. 5. Specific capacitance of OMC and OMCN-*x* (x=125, 150, 175, 200, 250, 275, 300) electrodes at different temperatures as a function of scan rate.

and the structure of the composites, which were affected by the hydrothermal temperature. The excellent properties of the nickel nitrate hydroxide hydrate encapsulated by an OMC are enhanced distinctly in the composite in comparison with the pure OMC electrode and other composites, as mentioned previously.

Fig. 5 shows the relationship between the specific capacitance and various scan rates of 5, 10, 20, 30 and 50 mV s^{-1} at different temperatures. As seen from Fig. 5, all the capacitance decreased with the increase of the scan rate at all temperatures, for which the internal resistance of the capacitor is responsible. In addition, OMCN-150, OMCN-175 and OMCN-125 exhibited more excellent performance, especially when the temperature is 150 °C, which indicates that the electrochemical performances of the supercapacitor were improved greatly with the changing of hydrothermal temperatures. The textural characteristics and the structure of the composites were affected by the hydrothermal temperature. The lower hydrothermal temperature led to the poorer crystallinity of the composite, which resulted in the better electrochemical performance. At the lowest scan rate of 5 mV s^{-1}, the specific capacitance of OMC and OMCN-150 is found to be 247 and 581 F g^{-1}, respectively. Based on the various hydrothermal temperatures of the composite, the capacitance of an OMCN-150 is about 2.4 times more than the pristine OMC at the scan rate of 5 mV s^{-1}. Furthermore, its specific capacitance is about 1.5 times of pristine OMC at the scan rate of 50 mV s^{-1}. In addition, an OMCN-*x* (x=200, 250, 275, 300) demonstrates an excellent rate capability due to the effect of hydrothermal temperature on the structure of the composite. Obviously, the temperature was further evaluated to 200 °C, namely, the electrochemical properties became poor, while nickel nitrate hydroxide hydrate disappears gradually. It should be mentioned that the high specific capacitance 581 F g^{-1} is more or less equal to the ideal electrode materials like RuO_2 and IrO_2. Recently, more and more researchers develop various alternatives as a replacement for RuO_2 and IrO_2, aiming to lower the cost of electrode material, while using environmentally friendly materials. We can assume that the novel composite OMCN-150 (nickel nitrate hydroxide hydrate/OMC composite) appears to be a promising electrode material for supercapacitor as a replacement for RuO_2 and IrO_2.

Since long cycle-life is the most vital criteria for a supercapacitor electrode, endurance tests for both types of electrode prepared in this study were undertaken by means of cycling the electrode voltammetrically between −0.2 and 0.5 V at a scan rate of 5 mV s^{-1} for 500 times. Fig. 6 gives the cycling tests of the OMCN-150 and OMC. Both the electrodes give highly stable cycle ability after 500 cycles; and at the termination of the test, the capacitance retention of pristine OMC and OMCN-150 electrodes is found to be 95.3% and 96.1%, respectively.

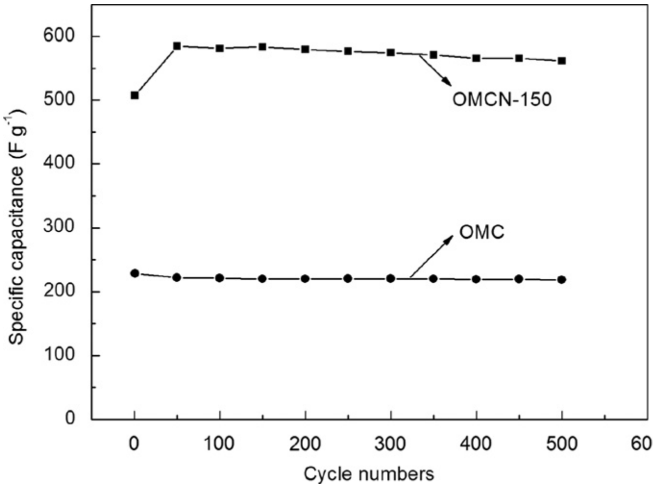

Fig. 6. Cycle-life of pristine OMC and OMCN-150 electrodes.

4. Conclusions

A series of high performance ordered mesoporous carbon (OMC)/nickel compounds composites were synthesized by a combination of incipient wetness impregnation and hydrothermal method for the first time. It is noteworthy that an OMC/nickel nitrate hydroxide hydrate composite exhibited more excellent performance (the capacitance retention of it is found to be 96.1% and about 2.4 (5 mV s^{-1}) and 1.5 (50 mV s^{-1}) times of the pristine OMC), which indicates that the electrochemical property of the supercapacitor was improved greatly with the changing of hydrothermal temperatures and as a new class of supercapacitor material noticeably broadens the scope of electrode material of the future. Further work is, however, clearly warranted to understand the dynamic electrochemical and structural changes occurring during hydrothermal treatment and the process of charge–discharge. Opportunities also exist for exploring other multivalent states of transition metal nitrate as a potential material for supercapacitors.

Acknowledgments

This work was financially supported by the Science and Technology Commission of Shanghai Municipality (No. 0952nm-02500) and the Scientific Research Foundation of Graduate School of Shanghai University of Engineering Science (No. B8909080116).

References

[1] A. Malak-Polaczyk, C. Matei-Ghimbeu, C. Vix-Guterl, E. Frackowiak, J. Solid State Chem. 183 (2010) 969–974.
[2] R. Ryoo, S. Joo, S. Jun, J. Phys. Chem. B 103 (1999) 7743–7746.
[3] H. Zhou, S. Zhu, M. Hibino, I. Honma, J. Power Sour. 122 (2003) 219–223.
[4] L. Li, H. Song, X. Chen, Electrochim. Acta 51 (2006) 5715–5720.
[5] C. Minchev, H. Huwe, T. Tsoncheva, D. Paneva, M. Dimitrov, I. Mitov, M. Fröba, Microporous Mesoporous Mater. 81 (2005) 333–341.
[6] Z. Guo, G. Zhu, B. Gao, D. Zhang, G. Tian, Y. Chen, W.W. Zhang, S.L. Qiu, Carbon 43 (2005) 2344–2351.
[7] V. Subramanian, H.W. Zhu, B.Q. Wei, Electrochem. Commun. 8 (2006) 827–832.

[8] J. Li, X. Wang, Q. Huang, S. Gamboa, P.J. Sebastian, J. Power Sour. 160 (2006) 1501–1505.
[9] S. Zhu, H. Zhou, M. Hibino, I. Honma, M. Ichihara, Adv. Funct. Mater. 15 (2005) 381–386.
[10] H. Huwe, M. Fröba, Carbon 45 (2007) 304–314.
[11] V. Srinvasan, J.W. Weidner, J. Electrochem. Soc. 144 (1997) L210–L213.
[12] Y.G. Wang, Y.Y. Xia, Electrochim. Acta 51 (2006) 3223–3227.
[13] W. Xing, F. Li, Z.F. Yan, G.Q. Lu, J. Power Sour. 134 (2004) 324–330.
[14] K.C. Liu, M.A. Anderson, J. Electrochem. Soc. 143 (1996) 124–130.
[15] N. Nagarajan, H. Humadi, I. Zhitomirsky, Electrochim. Acta 51 (2006) 3039–3045.
[16] H. Kim, T. Seong, J. Lim, W.I. Cho, Y.S. Yoon, J. Power Sour. 102 (2001) 167–171.
[17] L. Cao, L.B. Kong, Y.Y. Liang, H.L. Li, Chem. Commun. 14 (2004) 1646–1647.
[18] H. Bode, K. Dehmelt, J. Witte, Electrochim. Acta 11 (1966) 1079–1087.
[19] T.N. Ramesh, R.S. Jayashree, P.V. Kamath, S. Rodrigues, A.K. Shukla, J. Power Sour. 104 (2002) 295–298.
[20] Z. Chang, H. Tang, J.G. Chen, Electrochem. Commun. 1 (1999) 513–516.
[23] M.S. Wu, H.H. Hsieh, Electrochim. Acta 53 (2008) 3427–3435.
[24] Q.H. Huang, X.Y. Wang, J. Li, C.L. Dai, S. Gamboa, P.J. Sebastian, J. Power Sour. 164 (2007) 425–429.
[25] D. Zhao, J. Feng, Q. Huo, N. Melosh, G.H. Fredrickson, B.F. Chmelka, G.D. Stucky, Science 279 (1998) 548–552.
[26] Y. Shanmugam, F.Y. Lin, T.H. Chang, C.T. Yeh, J. Phys. Chem. B. 107 (2003) 1044–1047.
[27] H. Huwe, M. Fröba, Microporous Mesoporous Mater. 60 (2003) 151–158.